In-line production of a bi-circular field for generation of helically polarized high-order harmonics

Ofer Kfir, Eliyahu Bordo, Gil Ilan Haham, Oren Lahav, Avner Fleischer, and Oren Cohen

Citation: Applied Physics Letters **108**, 211106 (2016); doi: 10.1063/1.4952436
View online: http://dx.doi.org/10.1063/1.4952436
View Table of Contents: http://scitation.aip.org/content/aip/journal/apl/108/21?ver=pdfcov
Published by the AIP Publishing

In-line production of a bi-circular field for generation of helically polarized high-order harmonics

Ofer Kfir,[1,a)] Eliyahu Bordo,[1] Gil Ilan Haham,[1] Oren Lahav,[1] Avner Fleischer,[1,2] and Oren Cohen[1,a)]
[1]*Solid State Institute and Physics Department, Technion, Haifa 32000, Israel*
[2]*Department of Physics and Optical Engineering, Ort Braude College, Karmiel 21982, Israel*

(Received 9 January 2016; accepted 11 May 2016; published online 26 May 2016)

The recent demonstration of bright circularly polarized high-order harmonics of a bi-circular pump field gave rise to new opportunities in ultrafast chiral science. In previous works, the required nontrivial bi-circular pump field was produced using a relatively complicated and sensitive Mach-Zehnder-like interferometer. We propose a compact and stable in-line apparatus for converting a quasi-monochromatic linearly polarized ultrashort driving laser field into a bi-circular field and employ it for generation of helically polarized high-harmonics. Furthermore, utilizing the apparatus for a spectroscopic spin-mixing measurement, we identify the photon spins of the bi-circular weak component field that are annihilated during the high harmonics process. *Published by AIP Publishing.*
[http://dx.doi.org/10.1063/1.4952436]

Ultrashort pulses of extreme-UV and X-rays emerging from high harmonic generation (HHG) sources have been applied to many applications.[1–4] For many years, the polarization of bright HHG-based sources was limited to the linear region. Recently, bright circularly[5–8] and highly ellipticaly[9,10] polarized high harmonics were demonstrated and applied to downstream experiments.[6–10] In Refs. 5, 6, and 8, circular HHG was produced by driving the process with bi-circular field, that is, with bi-chromatic counter-rotating circularly polarized beams that jointly form a threefold shaped pulse.[11–14] The required complicated pump was produced by splitting and later combining the two spectral components in a Mach-Zehnder interferometer-like apparatus (e.g., Fig. 1 in Ref. 6). Thus, each pump beam propagates in a different arm of the interferometer, where its polarization and other properties are controlled independently. However, the Mach-Zehnder geometry has several significant drawbacks, including instability, polarization impurity, and time-consuming alignment.

Here, we present a simple and compact in-line (i.e., Mach-Zehnder-less) scheme for producing a bi-circular field for helically polarized HHG. We propose an apparatus, consisting of nonlinear crystal and achromatic quarter waveplate, which converts a quasi-monochromatic linearly polarized pump into a bi-circular field, composed of the fundamental field and its second harmonic (SH). We discuss the properties of our apparatus, including its superior polarization purity over a Mach-Zehnder-like geometry. We demonstrate that by simply inserting our apparatus into the pump beam path of an ordinary system for generation of linearly polarized high harmonics, the HHG spectrum changes from odd harmonics, which is typical to linearly polarized HHG to a set of harmonic pairs that is typical for circularly polarized HHG.[5–8,11–14] Furthermore, scanning the angle of the achromatic quarter waveplate yields a spectroscopic spin-mixing experiment in HHG, where the ellipticities of the two components of the bi-chromatic pump conjointly vary from linear through elliptic to circular. Analyzing such a scanning experiment with a relatively weak SH component, we identified all the spins of the annihilated SH photons. We believe that our apparatus will proliferate sources for circularly polarized high harmonics, in both the extreme-UV and soft-X-ray spectral regions, leading to exciting progress of ultrafast chiral phenomena.

Figure 1(a) displays schematically the conversion of a standard beamline for linear HHG into a beamline for circularly polarized HHG by inserting the apparatus in the beam path. Fig. 1(b) is a compact realization of the apparatus, which we name MAZEL-TOV for MAch-ZEhnder-Less for Threefold Optical Virginia spiderwort. Our standard setup for generating linearly polarized HHG consists of a linearly polarized pulsed laser beam that emerges from a Ti:Sapphire laser amplifier system (1 kHz, $\lambda = 770$ nm, $\sim$27 fs, 1.5 mJ). A lens (f = 500 mm) focuses the fundamental beam onto a jet of argon gas that is positioned in a vacuum chamber ($\sim 10^{-3}$–10^{-2} Torr). The HHG beam is separated from the pump beam by two thin aluminum foils (each 0.2 μm thick), and the HHG spectrum is analyzed by a spectrometer composed of a blazed grating, a toroidal mirror, and an extreme-UV CCD. In our MAZEL-TOV based setup, the fundamental pump laser pulse (illustrated as red, top left) is converted into a bi-circular field with effectively pure polarization and a joint focal point for the two fields. First, a portion of the energy of the linear s-polarized fundamental pulse, typically 10%–30%, is converted into a perpendicular p-polarized SH field ($\lambda = 394$ nm) in a beta-phase barium borate crystal (BBO, 0.2 mm, cutting angle 29.2° for type I phase matching). After the BBO, the power of the fundamental and SH beams was 1.05 W and 0.125 W, respectively. Placing the BBO after the focusing lens ensures that the wave front curvature of the converging fundamental laser beam is imprinted onto that of the SH field. Therefore, these two beams focus jointly to the same focal spot in the gas. Working with co-converging fundamental and SH removes

a)Authors to whom correspondence should be addressed. Electronic addresses: ofertx@technion.ac.il and oren@si.technion.ac.il

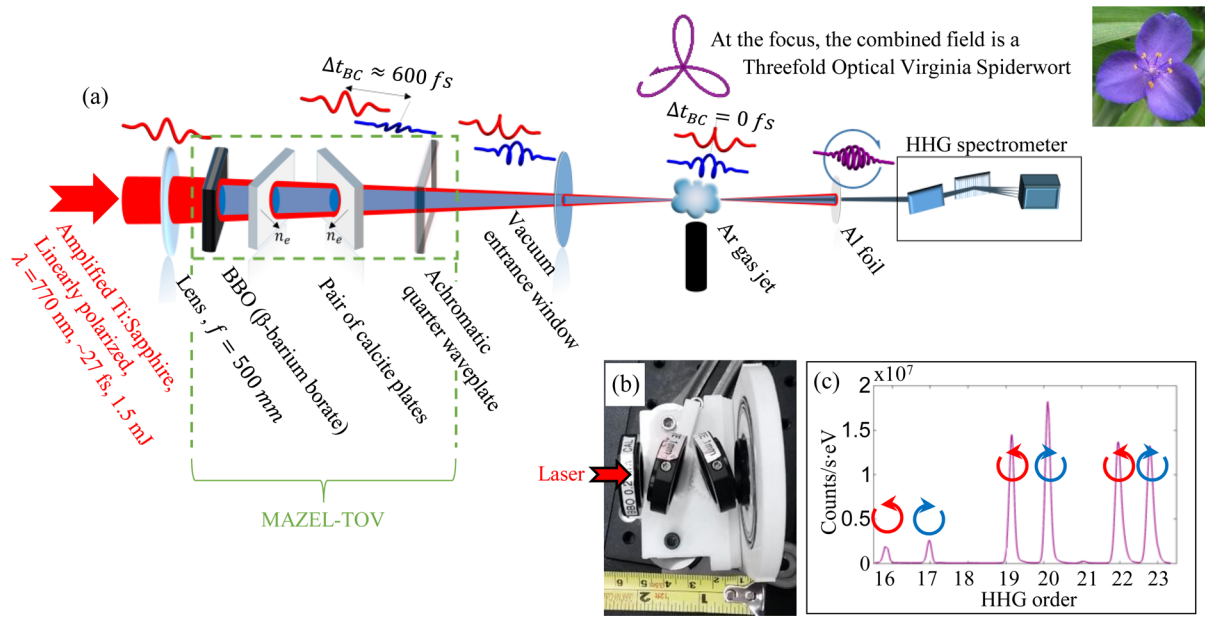

FIG. 1. (a) Scheme of simple and robust generation of high harmonics with controllable polarization (demonstration in supplemental movie clip[16]). Top right shows a threefold optical and a botanical Virginia Spiderwort. (b) A compact (2″ long) implementation of a MAZEL-TOV apparatus including a BBO (left), a pair of calcite plates, and a rotatable achromatic quarter waveplate (right). We added a ruler for scale and marked the laser entrance direction by a red arrow. (c) A recorded spectrum typical for circularly (or very highly elliptically) polarized HHG. The MAZEL-TOV apparatus (dashed green in (a)) is simply inserted into a standard system for generating linearly polarized HHG, where a lens (f = 500 mm) focuses a linear s-polarized fundamental beam onto a jet of argon gas in vacuum.

redundant spatial degrees of freedom which otherwise exist in a Mach-Zehnder configuration (e.g., spatial beam pointing and focal position of the two spectral components) while maintaining important degrees of freedom (e.g., relative time delay of the two spectral components and their polarizations). In other words, the foci of the two spectral components of the bi-chromatic field overlap spatially by default, in a robust manner. Second, the beam passes through a pair of calcite plates (55° cut with respect to the optical axis, 1 mm thick, AR coated) which pre-compensate for group delays induced by normally dispersive optics down the beam path. As illustrated in Fig. 1(a), the SH pulse (illustrated blue) precedes the fundamental (red) by $\Delta t_{BC} \sim 600$ fs as they emerge from the calcite plate pair.[15] This bi-chromatic delay, Δt_{BC}, is compensated for when the bi-chromatic field passes through the quarter waveplate and the vacuum chamber window, so the fundamental and SH pulses overlap temporally in the gas jet. The exact timing can be tuned by rotating the calcite plates around the axis perpendicular to the optical table. Rotating each plate within ±10° tunes its temporal compensation in the range of 145–300 fs, so the calcite plate pair supports delay range of 290–600 fs. We position the calcite pair with inversely rotated geometry and inward pointing extraordinary axis (marked n_e in Fig. 1(a), 55° tilt from the surface normal-vector) in order to cancel out any beam shifts caused by Snell's law and birefringent walk offs. Thus, the joint bi-chromatic focal spot is unperturbed by the plates' rotation. Third, the polarizations of the linear s-polarized fundamental and perpendicular p-polarized SH are converted to counter-rotating circular polarization by a single achromatic quarter-wave waveplate for the two spectral components. ($\lambda/4$ for 310 nm–1100 nm, B. Halle Nachfl. GmbH, RSU 1.4.20. We measured the waveplate retardation and obtained 0.258 and 0.240 waves for wavelengths 770 nm and 394 nm, respectively.) Once the polarizations are set to counter-rotating circular polarizations, stress-induced birefringence or tilting of optical element down the line may reduce the pump ellipticity. Therefore, the final element, an entrance window to the vacuum chamber (2 mm fused silica), is mounted with uniform stress distribution and perpendicular to the incoming beam. The absence of any polarization-modifying or tilted elements after the quarter waveplate allows for the polarization at the focal point to be controlled directly by the waveplate. This is an advantage compared to a Mach-Zehnder geometry, where a dichroic mirror tilted by 45° combines the two spectral components and may modify the circular polarization due to phase and amplitude differences between s- and p-polarization of the transmitted or reflected light. The HHG spectrum we observed with the MAZEL-TOV apparatus and argon gas jet (Fig. 1(c)) is typical for circularly polarized high harmonic.[5–8,11] It consists of pairs of counter-rotating harmonics, (16, 17), (19, 20), and (22, 23), where every third harmonic order, $q = 3m$, is suppressed (here 18 and 21). Harmonic orders $q = 3m + 1$ (here 16, 19, 22) rotate as the fundamental field (red circular arrows), while harmonic orders $q = 3m - 1$ (here 17, 20, 23) rotate as the SH field (blue circular arrows). q is the harmonic order defined by $q = 770\,\text{nm}/\lambda_{HHG}$, and m is an integer. The fact that the suppression of harmonic orders $3m$ is stronger in this work than in Refs. 5–8 suggests that the MAZEL-TOV apparatus yields HHG with higher level of circular polarization than Mach-Zehnder-based systems. The supplementary movie clip[16] displays that insertion of a MAZEL-TOV apparatus in the beam path changes the spectrum from evenly spaced odd-harmonics to a set of harmonic pairs, that is, from the typical spectrum of linearly polarized HHG to the spectrum of circularly (or very highly elliptically) polarized HHG.[5–8]

The use of birefringent (e.g., calcite) crystals, that in the MAZEL-TOV geometry are used primarily for temporal

compensation, can also be employed as de facto polarization purifiers for ultrashort pulses that drive extreme nonlinear optics experiments. When an ultrashort pulse enters a crystal and its polarization is dominantly along one crystal axis, yet it also includes a parasitic component along the orthogonal axis, the crystal can separate the two polarization components by introducing a delay of hundreds of femtoseconds between them. Extreme nonlinear processes pumped by such a field will be governed by the dominant pulse, which is now purely linearly polarized (notably, only time-resolved polarization measurements can sense this polarization purification). This temporal polarization purification can be useful in various schemes for HHG, e.g., to clean driving pulses from optical parametric amplifiers (OPA) or pulses with polarization impurities due to optical misalignments, etc. In the MAZEL-TOV geometry, an achromatic waveplate converts such an effectively purified perpendicularly polarized bi-linear pulse into a bi-circular pulse. The polarization purification effect is dramatic for bi-circular driving pulses because, in this case, the temporally shifted impurities are circularly or highly elliptically polarized, i.e., they cannot generate high harmonics even if their intensities are high.[17] Indeed, the HHG spectrum we observed (Fig. 1(c)) hardly changed when we added artificial polarization impurities by rotating the first calcite plate or the BBO of our MAZEL-TOV apparatus by up to 10° in the polarization plane of the pump. Thus, if a MAZEL-TOV apparatus is placed in the vacuum section of a HHG chamber (or even if only a calcite plate and an achromatic waveplate are placed in vacuum), then one can use popular birefringent vacuum windows from CaF_2 and Sapphire.

The MAZEL-TOV apparatus offers a spin-selective spectroscopic HHG scan: by rotating the angle of a single achromatic waveplate, we are now able to identify experimentally all the spin-mixtures that photons from a weak SH field contribute to HHG. For example, Fig. 2(a) shows a rich structure of the 16th harmonic order pumped by a bi-chromatic field composed of a fundamental field ($\lambda_1 = 770$ nm, 1.05 W) and its relatively weak SH ($\lambda_2 \approx 0.51\,\lambda_1$, 0.125 W). The SH central wavelength was set to $\lambda_2 \approx 0.51\,\lambda_1$ by tilting the BBO crystal, which spectrally tunes the phase matching window of the SH generation process. As in Ref. 5, the use of incommensurate frequencies allows us to identify the number of annihilated photons from each driver. Indeed, we identified three channels along the vertical (photon-energy) axis in Fig. 2(a): $(n_1 = 6, n_2 = 5)$, $(n_1 = 10, n_2 = 3)$, and $(n_1 = 14, n_2 = 1)$, where n_1 and n_2 correspond to the number of λ_1 and λ_2 annihilated photons. Notably, the intensity of channels increases with decreasing n_2, reflecting the fact that the SH component of the bi-circular field is significantly weaker than the fundamental one. Next, we discuss the structure along the horizontal (polarization) axis in Fig. 2(a) which we associate with spin-mixing conservation.[5,18] When the waveplate angle is at 45°, the two fields are circularly polarized with opposite helicity: the spin of the fundamental and SH photons is $+1$ and -1, respectively (in units of $\hbar$). At other angles, the two fields are elliptical (or linear) with the same ellipticity and perpendicular major axis (see color illustration at the top of Fig. 2(a)). In this case, HHG can be analyzed through mixing of four circularly polarized waves.[18] We describe each sub-channel by: $(n_{1+}, n_{1-}, n_{2+}, n_{2-})$, where n_{1+} and n_{1-} correspond to the number of λ_1 annihilated photons with $+1$ and -1 spin angular momentum, respectively, and similarly for n_{2+} and n_{2-} at λ_2. According to conservation of angular momentum, $n_{1+} - n_{1-} + n_{2+} - n_{2-} = \pm 1$, while conservation of energy gives rise to: $n_1 = n_{1+} + n_{1-}$, $n_2 = n_{2+} + n_{2-}$ and $16 = n_1 + 2n_2$. Consider sub-channels where none of n_{1+}, n_{1-}, n_{2+} and n_{2-} is zero, e.g., sub-channel (3,3,3,2). According to the conservation laws, all these sub-channels are allowed at all waveplate angles except for ±45°. So, how can we understand the observed structure in Fig. 2(a)? Is there any order in this structure? What are the observed peaks? The order is revealed by observing that the number of sub-channels in each channel in Fig. 2(a) is $n_2 + 1$, which is also the number of options for $n_{2+} = 0, 1, 2, \ldots, n_2$ (and also for n_{2-}). For example, for the channel $(n_1 = 6, n_2 = 5)$, we identify the following sub-channels: $(n_{2+}, n_{2-}) = (5,0)$, $(4,1)$, $(3,2)$, $(2,3)$, $(1,4)$, $(0,5)$. This pattern is consistent with all the harmonic spectra that we observed. For example, Fig. 2(b) shows the spectrogram from harmonic order 17. Thus, we conclude that we can identify the spins of the annihilated SH photons associated with each peak in the spectrogram, directly from the experimental measurement. In a sharp contrast, we do not identify the spins of the annihilated fundamental component. This feature indicates that the SH photons are acting as the bottleneck in the HHG process, where

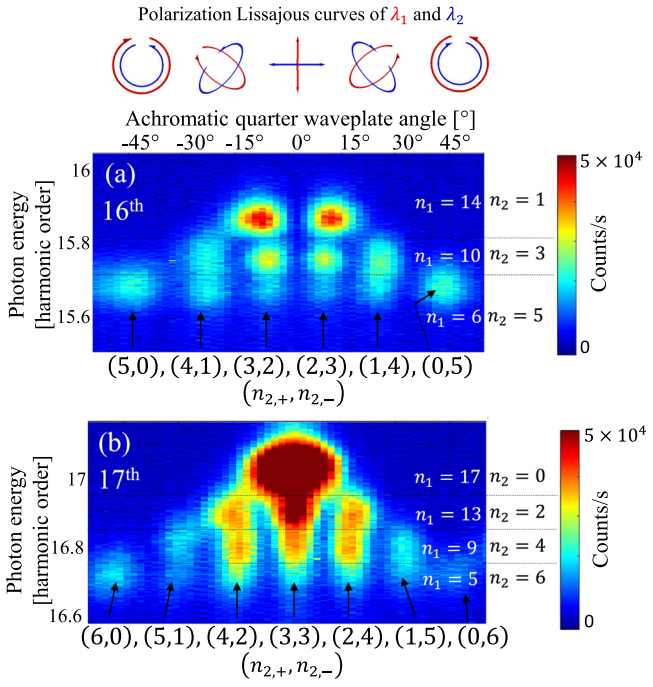

FIG. 2. Experimental spectrogram of the (a) 16th and (b) 17th harmonic orders showing rich energy and spin features. The incommensurate wavelength ratio $\lambda_2 = 0.51\lambda_1$ allows to identify the number of photons n_1 and n_2 annihilated from the fields λ_1 and λ_2, respectively. Since the SH field is weaker, channels with more fundamental photons (higher photon energy) are more intense. In the extreme case, the channel with $n_1 = 17$ and $n_2 = 0$ is exceeding the joint color scale of (a) and (b). Furthermore, the SH photons are the bottleneck for the HHG process, so the experimental spectrogram is sensitive to their spin mixture more than to that of the fundamental. When the field is circularly polarized (waveplate at ±45°), SH photons are available only with pure spin $+1$ or -1, that is, $(n_{2+}, n_{2-}) = (n_2, 0)$ or $(0, n_2)$, respectively. When the pump polarization is elliptical or linear, multiple channels with any combination of (n_{2+}, n_{2-}) are allowed. We are now able to identify separate channels corresponding to the spin-mixture of the SH photons, where both n_{2+} and n_{2-} vary from zero to their maximal value, n_2.

fundamental photons with appropriate spin are more abundant. Finally, we note that the observed spectra in Figs. 2(a) and 2(b) are highly symmetric, reflecting the reliable polarization control in a MAZEL-TOV (the control is less reliable in the Mach-Zehnder geometry as reflected by the asymmetric polarization scans in Fig. 3 of Ref. 5).

To conclude, we demonstrated conversion of a linearly polarized HHG source into a source of helically polarized HHG with an in-line MAZEL-TOV apparatus. The apparatus can be easily inserted and removed from the beam path of the fundamental pump laser, as shown in the supplementary movie clip,[16] and it offers robust operation, effective purified polarizations, and direct control over the polarization state of the bi-chromatic pumping field. We utilized this in-line apparatus for a chiral HHG spectroscopy and identified the contribution of the weak SH component to spin-mixing in HHG. The MAZEL-TOV method can be generalized to any source of two co-propagating perpendicularly polarized spectral components, whether longer or shorter wavelength than the fundamental and second harmonic demonstrated in this work. We believe this method offers a basic tool to support the growing interest for investigation of chiral dynamics[19,20] and other qualitative and quantitative aspects of chiral physics in the extreme-UV and X-ray spectral region.

This work was supported by the Israel Science Foundation (Grant No. 1225/14), the Israeli Center of Research Excellence "Circle of Light" supported by the I-CORE Program of the Planning and Budgeting Committee and The Israel Science Foundation, and the Wolfson foundation.

[1]J. Miao, T. Ishikawa, I. K. Robinson, and M. M. Murnane, Science **348**, 530 (2015).
[2]F. Krausz and M. I. Stockman, Nat. Photonics **8**, 205 (2014).
[3]S. Mathias, C. La-O-Vorakiat, P. Grychtol, P. Granitzka, E. Turgut, J. M. Shaw, R. Adam, H. T. Nembach, M. E. Siemens, S. Eich, C. M. Schneider, T. J. Silva, M. Aeschlimann, M. M. Murnane, and H. C. Kapteyn, Proc. Natl. Acad. Sci. U.S.A. **109**, 4792 (2012).
[4]K. M. Hoogeboom-Pot, J. N. Hernandez-Charpak, X. Gu, T. D. Frazer, E. H. Anderson, W. Chao, R. W. Falcone, R. Yang, M. M. Murnane, H. C. Kapteyn, and D. Nardi, Proc. Natl. Acad. Sci. U.S.A **112**, 4846 (2015).
[5]A. Fleischer, O. Kfir, T. Diskin, P. Sidorenko, and O. Cohen, Nat. Photonics **8**, 543 (2014).
[6]O. Kfir, P. Grychtol, E. Turgut, R. Knut, D. Zusin, D. Popmintchev, T. Popmintchev, H. Nembach, J. M. Shaw, A. Fleischer, H. Kapteyn, M. Murnane, and O. Cohen, Nat. Photonics **9**, 99 (2015).
[7]D. D. Hickstein, F. J. Dollar, P. Grychtol, J. L. Ellis, R. Knut, C. Hernández-García, D. Zusin, C. Gentry, J. M. Shaw, T. Fan, K. M. Dorney, A. Becker, A. Jaroń-Becker, H. C. Kapteyn, M. M. Murnane, and C. G. Durfee, Nat. Photonics **9**, 743 (2015).
[8]T. Fan, P. Grychtol, R. Knut, C. Hernández-García, D. D. Hickstein, D. Zusin, C. Gentry, F. J. Dollar, C. A. Mancuso, C. W. Hogle, O. Kfir, D. Legut, K. Carva, J. L. Ellis, K. M. Dorney, C. Chen, O. G. Shpyrko, E. E. Fullerton, O. Cohen, P. M. Oppeneer, D. B. Milošević, A. Becker, A. A. Jaroń-Becker, T. Popmintchev, M. M. Murnane, and H. C. Kapteyn, Proc. Natl. Acad. Sci. U.S.A **112**, 14206 (2015).
[9]A. Ferré, C. Handschin, M. Dumergue, F. Burgy, A. Comby, D. Descamps, B. Fabre, G. A. Garcia, R. Géneaux, L. Merceron, E. Mével, L. Nahon, S. Petit, B. Pons, D. Staedter, S. Weber, T. Ruchon, V. Blanchet, and Y. Mairesse, Nat. Photonics **9**, 93 (2015).
[10]G. Lambert, B. Vodungbo, J. Gautier, B. Mahieu, V. Malka, S. Sebban, P. Zeitoun, J. Luning, J. Perron, A. Andreev, S. Stremoukhov, F. Ardana-Lamas, A. Dax, C. P. Hauri, A. Sardinha, and M. Fajardo, Nat. Commun. **6**, 6167 (2015).
[11]S. Long, W. Becker, and J. K. McIver, Phys. Rev. A **52**, 2262 (1995).
[12]H. Eichmann, A. Egbert, S. Nolte, C. Momma, B. Wellegehausen, W. Becker, S. Long, and J. K. McIver, Phys. Rev. A **51**, R3414 (1995).
[13]D. B. Miloševic, J. Phys. B: At. Mol. Opt. Phys. **33**, 2479 (2000).
[14]D. B. Milošević and W. Becker, Phys. Rev. A **62**, 011403 (2000).
[15]For birefringent refractive indices of $CaCO_3$ (Calcite) see M. N. Polyanskiy, http://Refractiveindex.info (2015).
[16]See supplementary material at http://dx.doi.org/10.1063/1.4952436 for a movie clip of a MAZEL-TOV apparatus converting odd-harmonic spectrum, typical for linear harmonics, to a typical spectrum for circularly (or very highly elliptically) polarized HHG, where every third harmonic order is suppressed.
[17]M. Möller, Y. Cheng, S. D. Khan, B. Zhao, K. Zhao, M. Chini, G. G. Paulus, and Z. Chang, Phys. Rev. A **86**, 011401 (2012).
[18]E. Pisanty, S. Sukiasyan, and M. Ivanov, Phys. Rev. A **90**, 043829 (2014).
[19]K. Lin, X. Gong, Q. Song, Q. Ji, W. Zhang, J. Ma, P. Lu, H. Pan, J. Ding, H. Zeng, and J. Wu, J. Phys. B: At. Mol. Opt. Phys. **49**, 025603 (2016).
[20]O. Smirnova, Y. Mairesse, and S. Patchkovskii, J. Phys. B: At. Mol. Opt. Phys. **48**, 234005 (2015).